Application of Open Path Fourier Transform Infrared Spectroscopy (OP-FTIR) to Measure Greenhouse Gas Concentrations from Agricultural Soils

Cheng-Hsien Lin[1], Cliff T. Johnston[1], Richard H. Grant[1], and Albert J. Heber[2]

5 [1]Department of Agronomy, Purdue University, West Lafayette, IN 47907, United States
[2]Department of Agricultural and Biological Engineering, Purdue University, West Lafayette, IN 47907, United States

Correspondence to: Cheng-Hsien Lin (lin471@purdue.edu)

Abstract. Open-path Fourier transform infrared spectroscopy (OP-FTIR) has often been used to measure hazardous or trace gases from the "hot" point sources (e.g., volcano, industrial or agricultural facilities) but seldom used in the field-scale

10 source areas, such as soil emissions. OP-FTIR, the close-path mid-IR laser-based N_2O, and the nondispersive-IR CO_2 analyzers were used to measure the concentrations of greenhouse gases (e.g., N_2O and CO_2) emitted from agricultural soils over a period of 9-19th June in 2014. We developed a quantitative method of N_2O/CO_2 analysis that minimized the interferences from diurnal changes of humidity and temperature in order to measure N_2O/CO_2 concentrations accurately. Two chemometric multivariate models were developed, a classical least squares (CLS) and a partial least squares (PLS),

15 respectively. This study evaluated different methods to generate the single beam background spectra, and different spectral regions to determine N_2O/CO_2 concentrations from OP-FTIR spectra. A standard extractive method was used to measure the 'actual' path-averaged concentrations along an OP-FTIR optical path in situ, as a benchmark to assess the feasibilities of these quantitative methods. Within the absolute humidity of 5,000-20,000 ppmv and the temperature of 10-35 ℃, we found that the CLS model underestimated N_2O concentrations (Bias = -4.9±3.1 %) calculated from OP-FTIR spectra, and the PLS

20 model improved the accuracy of the calculated N_2O (Bias = 1.4±2.3 %). The bias of the calculated CO_2 was -1.0±2.8 % using the CLS model. These methods suggested that the changed ambient factors potentially led to biases in N_2O/CO_2 estimations from OP-FTIR spectra, and may help the OP-FTIR user to escape from the dependency of extractive methods used to calibrate the concentration determined by OP-FTIR.

1 Introduction

25 Agriculture contributes a substantial amount of greenhouse gas (GHG) emissions (e.g. N_2O, CO_2, and CH_4) to the global GHG budget (IPCC, 2007; Cole et al., 1997; Smith et al., 2008). Among these gases, N_2O is mainly emitted from agricultural soils, accounting for 38% of the global anthropogenic non-CO_2 GHG emissions from agricultural activities (Smith et al., 2007; US-EPA, 2006). N_2O is produced from biological reactions that transform available N in soils via microbial nitrification and denitrification (Mosier et al., 2004). Taking into account that the global warming potential value

Atmospheric
Measurement
Techniques
Discussions

of N_2O is 310, it is estimated that overall GHG emission from soils (based on CO_2 equivalents) is approximate 2500 MtCO$_2$-eq yr^{-1}. A significant fraction of soil N_2O emissions results from the use of nitrogen fertilizers in agricultural soils. In addition to contributing to the overall GHG burden of the atmosphere, N_2O emissions also represent a direct loss of the N applied to the field, contributing to the decreased nitrogen use efficiency (NUE) (Eichner, 1990; Ryden and Lund, 1980; Bremner et al., 1981). Also, soils play the role of a sink or a source for the atmospheric CO_2 (Paustian et al., 1997; Smith et al., 2008). Changing land use, especially agricultural-related uses such as tile drained and tilled managements, and agricultural lime application (e,g., $CaCO_3$ and $MgCa(CO_3)_2$) potentially become a large source of CO_2 released to the atmosphere via microbial decomposition of soil organic carbon (Smith, 2004; IPCC, 2007; Cole et al., 1997, West et al., 2005).

Chamber measurements have been the most common method to measure GHG emissions from soils (Denmead, 2008; Rochette and Eriksen-Hamel, 2008). Chamber measurements, however, are subject to significant limitations that lead to uncertainties and biases in the estimated GHG emissions. For instance, because chambers have a small footprint (~0.5 m^2) and generally wide sampling intervals (usually once a week), they are poorly suited to study the spatial and temporal variability of GHGs from agricultural soils (Laville et al., 1999; Rowlings et al., 2012; Schelde et al., 2012). Also, the increased wind turbulence substantially induced more gas transportation from soils to the atmosphere. Chamber methods unlikely consider the wind-induced effect into account, so likely resulting in underestimations for gas measurements (Denmead and Reicoshky, 2003; Poulsen et al., 2017; Pourbakhtiar et al., 2017).

Open-path Fourier transform infrared spectroscopy (OP-FTIR) is a non-intrusive sensing approach and capable of detecting multiple components simultaneously, acquiring real-time data at a relatively high temporal resolution (second to minutes), and providing path-averaged gas concentrations (Russwurm et al., 1991). OP-FTIR has been applied to measure atmospheric gases since the 1970s (e.g., hazardous air pollutants, fugitive volatile organic compounds (VOCs), and trace gases) (Herget and Brasher, 1980; Gosz et al., 1988; Russwurm et al., 1991; Bacsik et al., 2006; Briz et al., 2007; Lin et al., 2008). More recently, OP-FTIR has been increasingly applied to measure GHGs or other trace gases in agriculture, mostly in animal facilities (e.g., N_2O, CO_2, CH_4, and NH_3 from the swine or dairy production facility) (Childers et al., 2001; Loh et al., 2008; Bjorneberg et al., 2009; Barrancos, 2013; Naylor et al., 2016). Only a few studies, however, implemented OP-FTIR to measure gas emissions from vegetable production fields or fertilized soils (Bai et al., 2014 and 2018; Ni et al., 2015). Integrating OP-FTIR with the micrometeorological techniques (e.g., flux gradient (FG) or backward Lagrangian stochastic dispersion (bLS) methods) can measure gas fluxes from the field-scale source of interest with high temporal and spatial representatives that are less prone to artifacts induced by point-based sampling (Flesch et al., 2004 and 2016; Bai et al., 2014 and 2018; Ni et al., 2015). Moreover, the OP-FTIR combined with a scanning system can potentially be applied to horizontally or vertically survey numerous fields of interest and measure their gas emissions simultaneously (Flesch et al., 2016).

Despite these advantages, OP-FTIR also faces a number of challenges. In order to resolve the spectral features of GHGs, high spectral resolution (< 0.5 cm^{-1}) is required to resolve the rotation-vibrational absorption bands of the GHGs of interest (Griffiths and de Haseth, 2007). Calculating concentrations from FTIR spectra requires both a 'sample' single beam spectrum and a reference/background spectrum that does not contain spectral contributions from GHGs of interest, which is

5   not possible at the field scale (e.g., evacuation of the field); thus, mathematical methods have been developed which strip the spectral bands from a 'sample' single beam spectrum. This challenge requires the use of instrumental- or spectral-processing methods to create a background spectrum, and these methods are subject to biases to determine GHG concentrations (Griffiths and de Haseth, 2007; Russwurm and Childers, 1996). Furthermore, the atmosphere contains the high concentration of water vapour that interferes with the detection and quantification of GHGs of interest (Russwurm and Childers, 1996;

10   Horrocks et al., 2001; Briz et al., 2007; Smith et al., 2011). These challenges of data processes and the interferences from water vapour likely introduced biases and uncertainties in the GHG quantification. Using the error-prone concentration in flux prediction models (micrometeorological techniques) possibly leads to unknown uncertainties in the estimated gas fluxes. Thus, it is essential to develop a comprehensive quantitative method to improve and assure the quality of gas quantification using OP-FTIR.

15

Testing the feasibility of quantitative methods and qualities (accuracy and precision) of OP-FTIR is challenging because a trustable reference is required to validate the FTIR-derived concentrations. One of the most common approaches was to position a gas cell filled with known gas concentrations of interest in the optical path and test their quantitative methods (Russwurm et al., 1991; Horrocks et al., 2001; Smith et al., 2011). This approach, however, somewhat controlled the

20   environment and neglected the effect of the ambient interferences, such as water vapour, on the quality of gas quantification. The alternative approach is to compare the derived concentrations with ambient concentrations. The ambient concentration of a gas of interest can be determined by averaging the global background concentrations (e.g. $N_2O \sim 310$ ppbv or $CO_2 \sim 400$ ppmv) or measured from the gas samples that were collected along OP-FTIR path and analysed their concentrations using Lab-based gas chromatography (GC) (ASTM, 2013; Childers et al., 1995; Kelliher et al., 2002; Bai et al., 2014). The

25   experimental designs of these assessment approaches, either the point sampled setup or the low sampled frequency or both, became the major problem for cross-validating their OP-FTIR quantitative methods. Since the ambient concentrations likely fluctuate from place to place (e.g., different land uses) and in different timing (e.g., diurnal or seasonal variation), the spatial and temporal variations of the ambient concentration were potentially misconceived as "bias" in gas quantification. Up to now, only three studies continuously measured the real-time ambient concentration to logically cross-validate their

30   quantitative methods as well as data qualities under the fluctuated environmental factors (e.g., the dynamic water vapour), but none of the prior studies assess the methodology for quantifying N_2O concentrations (Briz et al., 2007; Frey et al., 2015; Reiche et al., 2014).

Therefore, the objectives of this study were to 1) develop a long-path gas sampling system that can continuously collect numerous gas samples along an optic path of OP-FTIR simultaneously and measure the path-averaged concentrations to evaluate the quantitative qualities of N_2O/CO_2 concentrations that were derived from OP-FTIR spectra, and 2) optimize the quantitative method, including post-data processing, analytical window selections, and chemometric multivariate algorithms

5   (i.e., classical least square and partial least square), that was less sensitive to the interference of ambient factors (i.e., humidity and temperature) and capable of determining N_2O and CO_2 concentrations accurately.

2 Materials and experimental methods

2.1 Site description

This study was conducted at the Purdue University Agronomy Center for Research and Extension near West Lafayette,

10   Indiana, the United States (86°56´ W, 40°49´ N, elevation 215 m). The experimental site was located between two fields (~3.5 hectares in each field) with a continuous corn system since 2013. Gas measurements began just after the anhydrous ammonia application with total N rate of 220 kg NH_3-N ha^{-1} on June 9th and ended on June 19th. The soils were classified as Drummer silty clay loam (fine-silty, mixed, mesic Typic Endoaquoll) with the bulk density of 1.6 $g \cdot m^{-3}$, organic matter of 3.4 %, soil pH of 6.0, and cation exchange capacity of 23 $cmol_c \cdot kg^{-1}$ (0-20 cm). During June 9-19th, the cumulative

15   precipitation was 57 mm, and the average soil temperature and moisture from the depth of 0-10 cm were 23($\pm$3) ℃ and 0.32($\pm$0.06) $cm^3 \cdot cm^{-3}$, respectively, which were determined by the on-site weather station.

2.2 Instrumentation setup (Fig.1)

The spectrometer was used a MIDAC Corporation monostatic open path FTIR air monitoring system (MIDAC Model2501-C, MIDAC Corporation, Irvine, CA). This instrument included the IR source, interferometer, transmitting/receiving

20   telescope, mercury cadmium telluride (MCT) detector and ZnSe optics. A mid-IR beam in the spectrometer passed through the atmosphere along an optical path and returned to the telescope after reflection from a retro-reflector to collect spectra that included the information of the gas of interest. A cube-corner retroreflector with 26 cubes was mounted on a retractable tripod with 150 m physical path length from the telescope, corresponding to an optical path length of 300 m.

25   Ambient concentrations of N_2O and CO_2 were also determined independently to assess the bias and precision. A difference frequency generation (DFG) mid-IR laser-based N_2O/H_2O analyzer (IRIS 4600, Thermo Fisher Scientific Inc., MA) and the non-dispersive infrared (NDIR) spectrometer CO_2/H_2O gas analyzer (LI-840, LI-COR Inc., NE) were used to measure N_2O and CO_2 concentrations of the sampled gases from a synthetic open path gas sampling system (S-OPS). The DFG laser-based N_2O analyzer determined N_2O concentrations in the mid-infrared wavelength with high precision of < 0.15 ppbv (1σ,

30   3 minute averaging). An NDIR CO_2 analyzer provided the high accuracy (< 1.5 % of reading) and low noise (< 1.0 ppmv) to determine CO_2 concentrations using single path, dual wavelength, and infrared detections system.

A 50 m long S-OPS combined with a gas sampling system (GSS) was used to collect gas samples along an optical path of OP-FTIR. An S-OPS consisted of 3/8 inch diameter Teflon® tubes and ten inlets fitted with one μm Teflon® filters. The flow rate of each inlet was adjusted by critical orifices in the inlets to 0.7 L·min^{-1} (±10 %). Gas samples were drawn through

5   an S-OPS line by a sampling pump in this GSS system at approximately 7 L·min^{-1} and collected into Teflon® ambient pressure chamber. Then, N_2O and CO_2 analyzers drew path-integrated air samples from the ambient pressure chamber (Heber et al., 2006), and the "actual" path-averaged concentrations of N_2O and CO_2 along the OP-FTIR path, which was used to benchmark N_2O/CO_2 concentrations calculated from the OP-FTIR spectrum. Temperature, relative humidity, and pressure in the ambient pressure chamber were also recorded every 30 seconds to monitor the functionality of the GSS.

10

Meteorological measurements of air temperature, relative humidity (HMP45C, Vaisala Oyj, Helsinki, Finland), and barometric pressure (278, Setra, Inc., Boxborough, MA) were at 1.5 m height of the mast located next to the S-OPS. The meteorological data were collected by a data logger (Model CR1000, Campbell Scientific, Logan, Utah), and averaged every 10 minutes. Wind speed and direction were acquired from a 3D sonic anemometer (Model 81000, RM Young Inc., Traverse

15   City, MI) mounted at 2.5 m on the meteorological mast and recorded at 5 min intervals. The recorded data were telemetered to the on-site instrumentation trailer.

2.3 General overview of N_2O/CO_2/water vapour concentrations, and air temperature

Figure 2 shows the 30-min averaged concentrations of ambient N_2O and CO_2 measured from the S-OPS, water vapour content and air temperature from the meteorological station during the period of 9-19th June in 2014. During this time

20   interval, 877 valid OP-FTIR spectra were collected with known concentrations of N_2O, CO_2, water vapour, and air temperature. To avoid the non-linear response of absorbance to the wide range of gas concentrations (Lamp et al., 1997), we selected ninety spectra containing 338±0.5 ppbv N_2O and ninety-three spectra containing 400±5 ppmv CO_2 which were measured from the S-OPS. These group of spectra covered broad ranges of water vapour content and air temperature. N_2O and CO_2 concentrations were calculated from these selected spectra using different quantitative methods.

25   ### 2.4 OP-FTIR data acquisition and QA/QC procedure

Each sampled spectrum was acquired by co-adding 64 single-sided interferograms (IFGs) at a nominal resolution of 0.5 cm^{-1}, which accounted for 32,000 data points were collected with the interval of 0.241 wavenumbers between data points, using the AutoQuant Pro4.0 software package (MIDAC Corporation, Irvine, CA). IFGs were converted to single beam (SB) spectra using a zero-filling factor of 1, triangular apodization, and Mertz phase correction. A stray light SB spectrum was

30   also acquired by pointing the transmitting/receiving telescope away from the retroreflector at the beginning of the experiment every day using the same parameters (Russwurm and Childers, 1996). Each sampled SB spectrum was stray light

corrected by subtracting the stray light SB spectrum from the sampled SB spectrum before converting to the absorbance spectrum.

The IFGs and corresponding SB spectra were influenced by ambient factors that included wind-derived vibrations,
5 scintillation induced by air mixing, water vapour content, dust accumulation and condensation on the retro-reflector. Criteria of quality assurance were based on the inspection of the IFG and the SB spectrum, which are followed the standard guideline in the MIDAC instrumentation manual and the FTIR open-path monitoring guidance documents (Russwurm and Childers, 1996) with the supplement criteria published by Childers et al. (2001b) and Shao et al. (2007) to acquire the high-quality spectrum. The maximum and minimum of the centerburst of the IFG were controlled between approximately 0.61-1.14 Volts
10 based on the physical path length of 150 m. IFG centerburst signals > 2.25 Volts were rejected to avoid a non-linear response of the MCT detector.

2.5 Spectral analyses

2.5.1 An absorbance spectrum converted from a single beam (SB) spectrum

In order to calculate a concentration for a given solute, a stray-light corrected SB spectrum is ratioed against an SB
15 background spectrum (GHGs-free) to produce an absorbance spectrum from which the gas concentration is determined using the Beer-Lambert law. As discussed earlier, OP-FTIR measurements do not permit the collection of a background spectrum that is 'free' of GHGs. Two different approaches were used in this study to overcome this constraint. Both methods required a 'normal' SB spectrum corresponding to the path length of interest that was then mathematically manipulated to produce a background spectrum. A representative field SB spectrum and the regions of interest for each of GHGs are shown in Figure
20 3(a). For the "zapped" background method, a background (zap-bkg) was obtained by drawing a straight line between two selected points which removed, or 'zapped,' any spectral contributions below the line using OMINC Macro Basic 8.0 commercial software (Thermo Fisher Scientific, Inc.). This is illustrated for the N_2O region of interest in Figure 3(b), with the two points and the line labeled as 'zapped' background. For the zap-bkg method, we selected one quality SB spectrum every day to create a zap-bkg, and all of the sampled SB spectra collected from one day were converted to absorbance
25 spectra using this zap-bkg. Another method, referred to as the 'synthetic' background method, was generated from this same original SB spectrum using IMACC software (Industrial Monitoring and Control Corp., Texas). In this case, numerous points in the 'non-absorbing' region of the SB spectrum were selected as 'base points,' and a high-order fitting function was used to construct a background spectrum. An example in the N_2O region is illustrated in Figure 3(b) and is labeled 'synthetic' background (syn-bkg). The mathematically manipulated SB spectra were used as background files to convert the sampled
30 SB spectra into absorbance spectra (Fig.3c and 3d). For the syn-bkg method, all data points were stored as one data file, and this file was applied to each sampled SB spectrum to create its syn-bkg. Since the selected points determined the curvature of the syn-bkg SB spectrum, it is critical to choose the data points that do not introduce any distortion (e.g. artificial dips and

peaks) into the curvature of the syn-bkg. In general, we avoided selecting data points within the absorption feature of interest (e.g. 2170-2224 cm^{-1} for N_2O analysis), and an adequate number of data points was used to fit the curvature of the SB spectrum as long as we can produce a smooth function (Russwurm and Childers, 1996). Adding too many data points may lead to the artificial distortion in a syn-bkg. Because the syn-bkg is one of the recommended methods used in the spectral

5 analysis (ASTM, 2013), this method was used to assess the feasibility of the zap-bkg method.

2.5.2 Gas quantifications: Multivariate models and spectral window selections

Based on Beer-Lambert law, we used reference spectra to predict gas concentrations from field absorbance spectra. In this study, we used classical least squares (CLS) and partial least squares (PLS) regressions to calculate N_2O and CO_2 concentrations. The details of these two methods are described as follows.

10

- CLS prediction model: Each of the reference spectra used in the CLS model only contained one gas component (e.g. N_2O, CO_2, or water vapour), and these reference spectra were generated from the high-resolution transmission molecular absorption (HITRAN) database (Rothman et al., 2005). The CLS model (AutoQuant Pro4.0) predicted gas concentrations from the field absorbance spectra converted using the zap-bkg method. In addition, CLS spectra were

15 also calculated using the IMACC software to predict gas concentrations from the spectra converted by the syn-bkg method. The non-linear function between the actual and predicted gas concentrations of the reference spectra was selected in the CLS model in both quantitative packages.

- PLS prediction model: Each of the reference spectra used in the PLS model had multiple gas components (e.g. an

20 N_2O/H_2O mixing spectrum). Gas samples were delivered to a multi-pass gas cell (White cell) with an optical path length of 33 m (Model MARS-8L/40L, Gemini Scientific Instruments, CA). Spectra were collected by a laboratory-based FTIR spectrometer (Nexus 670, Thermo Electron Corporation, Palatine, IL), including globar IR source, KBr beam splitter, and a mercury cadmium telluride High D* (MCT-High D*) detector. The FTIR was purged with dry air (-20 ℃ dew point) produced from a zero air generator (Model 701H, Teledyne, CA). N_2O was diluted with ultra-pure nitrogen

25 gas using a diluter (Series 4040, Environics Inc, CT), and the water vapour content was controlled by a Nafion tube contained within a sealing container of the saturated water vapour. Temperature and humidity were monitored using a Vaisala model HMT 330 humidity and temperature transmitter (Vaisala Oyj, Helsinki, Finland). N_2O concentrations were diluted from 30 ppmv to 0.3, 0.4, 0.5, 0.6 and 0.7 ppmv mixing with the relative humidity of 20, 40, 60, and 80 % at 303 K. Spectra were acquired at 0.5 cm^{-1} resolution, averaged from 64 sample scans with triangular apodization. A

30 total of 60 spectra of N_2O/H_2O mixing gases were used to build the PLS model using TQ Analyst software Version 8.0 (Thermo Fisher Scientific, Inc.) In order to avoid over-fitting the models, the optimum of factors used in PLS models were determined by cross-validation and justified by the prediction residual error sum of squares (PRESS) function. The

correlation between the known and the PLS-predicted concentrations was used to quantify N_2O from the field absorbance spectrum converted by syn-bkg within given spectral windows.

- Spectral window selections: The window selection (Fig. 4) was critical because of the interferences of water vapour. While a broader window contained more information of the gas of interest and potentially improved the spectral fit between the modeled and sampled spectra and the quantitative accuracy, it also included more features of water vapour and led to biases in gas quantifications. On the other hand, a narrow window can minimize the interfering effect of the uninteresting gases but may reduce the spectral information of the targeted gas which led to biases in gas calculations (e.g. underestimation for the gas quantification). The window used for N_2O quantifications was from 2130 to 2224 cm^{-1} that mainly includes the absorbance features of N_2O (P-branch) and water vapour, and we also selected different regions for calculating N_2O concentrations. For CO_2, the spectral windows of 2070-2085 cm^{-1} and 722-800 cm^{-1} (not shown) contains the features of CO_2 and water vapour (Rothman et al., 2005). We selected the multi-windows to calculate CO_2 concentrations and assessed the effect of water vapour on gas predictions.

2.6 The accuracy of the FTIR-calculated concentration and statistical analysis

Bias, the relative error between the S-OPS and OP-FTIR measured N_2O/CO_2, indicated the accuracy of the calculated N_2O and CO_2 concentrations using different spectral analyses (i.e. background types, multivariate models, and spectral windows) and can be calculated following Eq. (1):

$$Bias = \frac{(x_i - x_t)}{x_t} \times 100\% \tag{1}$$

, where x_i is the N_2O or CO_2 concentration calculated from the OP-FTIR spectrum, and x_t is the known N_2O or CO_2 concentration measured from the S-OPS. The calculated concentrations were statistically analysed by ANOVA procedures and protected least significant difference (LSD) (α=0.05) (SAS 9.3; SAS Institute Inc., 2012).

3 Results and discussion

3.1 Quantitative methods (SB backgrounds, spectral windows, and multivariate models)

Both SB background methods, zap-bkg and syn-bkg, respectively, were used to convert the sampled SB spectra to absorbance spectra for gas quantifications. Various windows were used to calculate gas concentrations from the field-measured OP-FTIR spectrum using CLS and PLS models. A series of OP-FTIR spectra acquired from broad ranges of humility (i.e., 5,000-20,000 ppmv water vapour) and temperature (10-35 ℃) were used to calculate N_2O and CO_2 concentrations. Within these ranges, the mean bias (%) indicated the accuracy of the calculated N_2O or CO_2 and the standard deviation (SD) referred to the sensitivity of the quantitative method to the changed water vapour and air temperature.

3.2 Nitrous oxide (338 ppbv)

Generally, the accuracy of the calculated N_2O concentration (mean bias) was improved by narrowing the spectral window because of the lessened water absorption features. In the CLS model, the broadest window (W_N1: 2170-2223.7 cm^{-1}) (Fig. 4) led to an underestimate of 10.7($\pm$2.3) % in N_2O calculations from the absorbance spectra that were converted by zap-bkg,

5 and this bias can be reduced using W_N2 (2188.5-2223.7 cm^{-1}) (i.e. 9.1$\pm$2.5 % underestimate). Likewise, W_N1 led to an underestimate of 8.1($\pm$2.6) % in N_2O calculations using syn-bkg, and this bias was reduced using W_N3 (2215.8-2223.7 + 2188.5-2204.1 cm^{-1}) (i.e. 5.6$\pm$2.6 % underestimate). Although narrowing the window mitigated the features as well as interferences of water vapour, it also lost the information of N_2O and potentially resulted in a great bias to predict N_2O concentrations if the analytical window was over confined. The most confined window (W_N4: 2188.5-2204.1 cm^{-1}) used in

10 the CLS model gave rise to greater biases in both zap- and syn-bkg procedures. Beside W_N1 (2170-2223.7 cm^{-1}), the P-branch feature of N_2O extended from 2130 to 2223.7 cm^{-1}, and we also used this entire region to calculate the N_2O concentration. In CLS model, the window of 2130-2223.7 cm^{-1} showed the minimum mean bias of -0.4% of the calculated N_2O concentrations using syn-bkg (data not shown); however, this window was sensitive to a water vapour interference and led to the highest variability in N_2O estimations (i.e., -0.4$\pm$5.3 %). As previously mentioned, it was crucial to generate a

15 reasonable background for the spectral analysis. The N_2O concentration calculated from the absorbance converted by syn-bkg was more accurate than zap-bkg (Fig. 5). In the CLS model, the bias of the calculated N_2O concentration using syn-bkg was significantly lower than zap-bkg based on the same spectral window (W_N1-3; P-values < 0.05) (Fig. 5). For N_2O quantification, we only used the P-branch of N_2O (2130-2223.7 cm^{-1}) to calculate N_2O concentrations because the R-branch feature of N_2O (2224-2280 m^{-1}) was strongly overlapped by the feature of CO_2 (2224-2450 cm^{-1}) in field spectra. Syn-bkg

20 better simulated the appropriate SB background over P- and R-branches of N_2O than zap-bkg which simply removed the P-branch of N_2O. Thus, syn-bkg can generate the N_2O absorbance (P-branch) without losing N_2O absorbance intensity (Fig. 3d) as well as the accuracy of the calculated N_2O.

The syn-bkg method, and the integrated window of 2215.8-2223.7 cm^{-1} and 2188.7-2204.1 cm^{-1} (W_N3) were considered as

25 the optimal combination for N_2O quantifications using the CLS models (i.e., lowest bias = -5.6$\pm$2.6 % in CLS, Fig.5b). This optimal combination was also used in the PLS model to predict N_2O concentrations. The mean bias of the calculated N_2O reduced from -5.6 % (CLS model) to -0.3 % (PLS model) (Fig. 5c). As compared to the CLS model, the PLS model significantly improved the accuracy of the calculated N_2O (P < 0.05) because the PLS algorithm can extract useful latent factors from the N_2O/H_2O mixing spectra (e.g. the contribution of water vapour to N_2O). The PLS model, however, led to

30 higher variability in the calculated N_2O than the CLS model based on the same window (Fig. 5c), indicating that the PLS model was more sensitive to the changed environment than the CLS model.

3.3 Carbon dioxide (400 ppmv)

For CO_2 estimations, three spectral windows were used in 2070-2085 cm^{-1} (Fig. 4c). The accuracy of the calculated CO_2 concentrations was also improved by narrowing the spectral window (Fig. 6). In the CLS model, the broadest window (W_C1: 2070-2084 cm^{-1}) led to an underestimate of 6.4($\pm$4.1) % in CO_2 calculations using zap-bkg. This bias reduced by narrowing the window to W_C2 (2075.5-2084 cm^{-1}) (i.e. 0.1$\pm$4.2 % underestimate). The calculated bias of CO_2 concentrations was -4.7($\pm$2.4) % using W_C1 and syn-bkg. This bias can be reduced to -0.3($\pm$2.4) % using W_C2. The most confined window (W_C3: 2075.5-2080.5 cm^{-1}) resulted in greater biases than W_C2, and particularly in conjunction with zap-bkg (i.e. 3.2$\pm$3.4 % bias) (Fig. 6). Thus, the range from 2075.5 to 2084 cm^{-1} (W_C2) was considered as the optimal window for CO_2 estimations (Fig. 4).

Zap-bkg conjoined with the optimal window (i.e. W_N3 or W_C2) in the CLS model led to greater underestimates in N_2O than CO_2 calculations (Bias: -10$\pm$2.3%, Fig.5a vs. -0.1$\pm$4.2%, Fig.6a). Since the absorbance features of CO_2 at 2076.9 cm^{-1} (the band center) was less complicated than the P-branch of N_2O from 2170 to 2224 cm^{-1}, the CO_2 absorbance converted by zap-bkg was similar with syn-bkg (Fig. 3c and 3d). Therefore, the calculated bias (Fig. 6) showed that there was no significant difference between zap- and syn-bkg methods for CO_2 concentration calculations. Generally speaking, zap-bkg showed a similar trend with syn-bkg by narrowing the spectral window. Zap-bkg led to the higher variability in the calculated CO_2, indicating that simply removing the CO_2 feature by the linear function potentially resulted in biases for CO_2 quantification.

The other potential region for CO_2 quantification was within 722-800 cm^{-1} (the R-branch of CO_2 v_2 band, Fig. 3a). Various windows were examined to calculate CO_2 concentration using the CLS model in this region, and the CO_2 concentrations were 40-70 % underestimated no matter which window was used in conjunction with zap-bkg. The minimum calculated mean bias was -9.0($\pm$2.9) % by incorporating two windows of 723-727.7 cm^{-1} and 732-738.5 cm^{-1} in conjunction with syn-bkg (data not shown). As compared with the results from 2070-2084 cm^{-1} (Fig. 4c), 722-800 cm^{-1} window resulted in a significant underestimations in CO_2 calculations because 1) more water vapour features interfered with the R-branch of CO_2 features in 722-800 cm^{-1} than CO_2 in 2070-2084 cm^{-1}, and 2) it was difficult to simulate the appropriate background at the low wavenumber region in the SB spectrum.

3.4 Diurnal N_2O/CO_2 estimations

The optimal quantitative approach of leading to the minimum bias in N_2O estimations was to use syn-bkg and W_N3 window in the PLS model (Fig. 5c); the optimal approach for CO_2 estimations was to use the syn-bkg procedure and W_C2 in the CLS model (Fig. 6b). These optimized methods were used to estimate the N_2O and CO_2 concentrations from the OP-FTIR spectra collected from 9th to 19th in June 2014 (Fig. 7). The diurnal fluctuation in N_2O and CO_2 concentrations were corresponding to the diurnal changes of the wind speed and air temperature. The higher N_2O/CO_2 concentrations were usually measured during the night because of N_2O and CO_2 accumulations. The accumulation of N_2O/CO_2 occurred near the ground when

turbulent mixing was low, resulting from the decreasing buoyancy from the ground surface (i.e. a stable atmosphere). The greater density of air parcel due to the decreasing temperature also led to the gas accumulation. The diurnal variation in CO_2 was greater than N_2O (Fig. 7b), and we hypothesized because of the multiple sources of CO_2. N_2O was mostly produced from soils via microbial nitrification and denitrification, but CO_2 was emitted via soil respiration (including microbes and
5   corn root) as well as the respiration from grass and corn leaves.

Mixing of the surface layer of the air tended to result in greater homogeneity along the optical path. Under low wind speed, the presumably poorly-mixed air increased the variability of the path-averaged N_2O/CO_2 concentrations along the optical path, resulting in the difference between the 50 m S-OPS and the 150 m OP-FTIR. The calculated biases of N_2O and CO_2
10   were 1.3($\pm$2.6) % (n=363) and -0.7($\pm$6.0) % (n=327), respectively, while the mean wind velocity ranged from 0.1 to 8.4 m·s^{-1} (Fig. 7). The variability of the calculated biases of N_2O and CO_2 were reduced when the data that were collected under the low wind speed (<1.7 m·s^{-1}) were excluded, i.e. $bias_{N_2O}$=1.4$\pm$2.3 % (n=295) and $bias_{CO_2}$=-1.0$\pm$2.8 % (n=269).

4 Conclusion

We have developed various methods to quantify concentrations of nitrous oxide and carbon dioxide using open-path FTIR
15   based on combinations of single beam backgrounds (i.e. zap-bkg and syn-bkg), analytical windows, and chemometric multivariate calibration models (i.e. CLS and PLS). It is challenging to generate the P-branch N_2O absorbance within 2170-2223.7 cm^{-1} to predict N_2O accurately but feasible to generate CO_2 absorbance in 2075.5-2084 cm^{-1} for CO_2 prediction using the zap-bkg method. The principle for selecting spectral window is to use the region with less water vapour features, yet over confining the analytical region may lead to biases in gas predictions. The CLS model, the most common approach used for
20   gas retrievals in OP-FTIR commercial packages, underestimates N_2O concentrations but can predict CO_2 accurately within the absolute humidity of 5,000-20,000 ppmv and the temperature of 10-35 ℃. In this study, the optimal method for N_2O quantification is to use the combination of syn-bkg, two bands window (2188.7-2204.1 + 2215.8-2223.7 cm^{-1}), and the PLS model (N_2O bias = 1.4$\pm$2.3 %). The optimal method for CO_2 quantification is to use the combination of syn-bkg, 2075.5-2084 cm^{-1} window, and the CLS model (CO_2 bias = -1.0$\pm$2.8 %). We provide comprehensive methods of N_2O/CO_2 analyses
25   for the increasing OP-FTIR users who are interested in greenhouse gas emissions from agricultural fields.

Atmospheric
Measurement
Techniques
Discussions

Open Access

EGU

References

ASTM International.: ASTM E1865-97(2013) Standard Guide for Open-Path Fourier Transform Infrared (OP/FT-IR) Monitoring of Gases and Vapors in Air, West Conshohocken, PA, doi:10.1520/E1865-97R13, 2013.

ASTM International.: ASTM E1982-98(2013) Standard Practice for Open-Path Fourier Transform Infrared (OP/FT-IR) Monitoring of Gases and Vapors in Air, West Conshohocken, PA, doi:10.1520/E1982-98R13, 2013.

Bacsik, Z., Komlosi, V., Ollar, T., and Mink, J.: Comparison of open path and extractive long-path FTIR techniques in detection of air pollutants, Appl. Spectrosc. Rev., 41, 77-97, doi:10.1080/05704920500385494, 2006.

Bai, M., Suter, H., Lam, S. K., Sun, J. L., and Chen, D. L.: Use of open-path FTIR and inverse dispersion technique to quantify gaseous nitrogen loss from an intensive vegetable production site, Atmos. Environ., 94, 687-691, doi:10.1016/j.atmosenv.2014.06.013, 2014.

Bai, M., Suter, H., Lam, S. K., Davies, R., Flesch, T. K., and Chen, D. L.: Gaseous emissions from an intensive vegetable farm measured with slant-path FTIR technique, Agric. For. Meteorol., 258, 50-55, doi:10.1016/j.agrformet.2018.03.001, 2018.

Barrancos, J., Briz, S., Nolasco, D., Melian, G., Padilla, G., Padron, E., Fernandez, I., Perez, N., and Hernandez, P. A.: A new method for estimating greenhouse gases and ammonia emissions from livestock buildings, Atmos. Environ., 74, 10-17, doi:10.1016/j.atmosenv.2013.03.021, 2013.

Bjorneberg, D. L., Leytem, A. B., Westermann, D. T., Griffiths, P. R., Shao, L., and Pollard, M. J.: Measurement of atmospheric ammonia, methane, and nitrous oxide at a concentrated dairy production facility in southern Idaho using open-path FTIR spectrometry, Trans. ASABE, 52, 1749-1756, 2009.

Bremner, J. M., Breitenbeck, G. A., and Blackmer, A. M.: Effect of nitrapyrin on emission of nitrous oxide from soil fertilized with anhydrous ammonia, Geophys. Res. Lett., 8, 353-356, doi:10.1029/GL008i004p00353, 1981.

Briz, S., de Castro, A. J., Díez, S., López, F., and Schäfer, K.: Remote sensing by open-path FTIR spectroscopy. Comparison of different analysis techniques applied to ozone and carbon monoxide detection, J. Quant. Spectrosc. Radiat. Transf., 103, 314-330, doi:10.1016/j.jqsrt.2006.02.058, 2007.

Childers, J. W., Russwurm, G. M., and Thompson, E. L.: Quality assurance considerations in a long-term FTIR monitoring program, Proc. SPIE 2365, Optical Sensing for Environmental and Process Monitoring, doi: 10.1117/12.210812, 1995.

Childers, J. W., Thompson, E. L., Harris, D. B., Kirchgessner, D. A., Clayton, M., Natschke, D. F., and Phillips, W. J.: Multi-pollutant concentration measurements around a concentrated swine production facility using open-path FTIR spectrometry, Atmos. Environ., 35, 1923-1936, doi:10.1016/s1352-2310(00)00545-8, 2001a

Childers, J. W., Thompson, E. L., Harris, D. B., Kirchgessner, D. A., Clayton, M., Natschke, D. F., and Phillips, W. J.: Application of standardized quality control procedures to open-path Fourier transform infrared data collected at a concentrated swine production facility, Environ. Sci. Technol., 35, 1859-1866, doi:10.1021/es001744f, 2001b.

Atmospheric
Measurement
Techniques
Discussions

Cole, C. V., Duxbury, J., Freney, J., Heinemeyer, O., Minami, K., Mosier, A., Paustian, K., Rosenberg, N., Sampson, N., Sauerbeck, D., and Zhao, Q.: Global estimates of potential mitigation of greenhouse gas emissions by agriculture, Nutr. Cycl. Agroecosyst., 49, 221-228, doi:10.1023/a:1009731711346, 1997.

Denmead, O., and Reicosky, D.: Tillage-induced gas fluxes: comparison of meteorological and large chamber techniques, Proc. ISTRO, 16, 357-363, 2003.

Denmead, O. T.: Approaches to measuring fluxes of methane and nitrous oxide between landscapes and the atmosphere, Plant Soil, 309, 5-24, doi:10.1007/s11104-008-9599-z, 2008.

Eichner, M. J.: Nitrous Oxide Emissions from Fertilized Soils: Summary of Available Data, J. Environ. Qual., 19, doi:10.2134/jeq1990.00472425001900020013x, 1990.

Flesch, T. K., Wilson, J. D., Harper, L. A., Crenna, B. P., and Sharpe, R. R.: Deducing ground-to-air emissions from observed trace gas concentrations: A field trial, J. Appl. Meteorol., 43, 487-502, doi:10.1175/1520-0450(2004)043<0487:dgefot>2.0.co;2, 2004.

Frey, M., Hase, F., Blumenstock, T., Gross, J., Kiel, M., Tsidu, G. M., Schafer, K., Sha, M. K., and Orphal, J.: Calibration and instrumental line shape characterization of a set of portable FTIR spectrometers for detecting greenhouse gas emissions, Atmos. Meas. Tech., 8, 3047-3057, doi: 10.5194/amt-8-3047-2015, 2015.

Flesch, T. K., Baron, V. S., Wilson, J. D., Griffith, D. W. T., Basarab, J. A., and Carlson, P. J.: Agricultural gas emissions during the spring thaw: Applying a new measurement technique, Agric. For. Meteorol., 221, 111-121, doi:10.1016/j.agrformet.2016.02.010, 2016.

Gosz, J. R., Dahm, C. N., and Risser, P. G.: Long-Path FTIR Measurement of Atmospheric Trace Gas Concentrations, Ecology, 69, 1326-1330, doi:10.2307/1941630, 1988.

Griffiths, P. R., and de Haseth, J. A.: Fourier transform infrared spectrometry, John Wiley & Sons, 2007.

Heber, A. J., Ni, J. Q., Lim, T. T., Tao, P. C., Schmidt, A. M., Koziel, J. A., Beasley, D. B., Hoff, S. J., Nicolai, R. E., Jacobson, L. D., and Zhang, Y. H.: Quality assured measurements of animal building emissions: Gas concentrations, J. Air Waste Manage. Assoc., 56, 1472-1483, doi:10.1080/10473289.2006.10465680, 2006.

Herget, W. F., and Brasher, J. D.: Remote Fourier transform infrared air pollution studies, Opt. Eng., 19, 194508-194508-, doi:10.1117/12.7972551, 1980.

Horrocks, L. A., Oppenheimer, C., Burton, M. R., Duffell, H. J., Davies, N. M., Martin, N. A., and Bell, W.: Open-path Fourier transform infrared spectroscopy of SO_2: An empirical error budget analysis, with implications for volcano monitoring, J. Geophys. Res.-Atmos., 106, 27647-27659, doi:10.1029/2001jd000343, 2001.

Kelliher, F. M., Reisinger, A. R., Martin, R. J., Harvey, M. J., Price, S. J., and Sherlock, R. R.: Measuring nitrous oxide emission rate from grazed pasture using Fourier-transform infrared spectroscopy in the nocturnal boundary layer, Agric. For. Meteorol., 111, 29-38, doi:10.1016/s0168-1923(02)00007-2, 2002.

Lamp, T., Radmacher, M., Weber, K., Gartner, A., Nitz, R., and Broker, G.: Calibration of an open-path FTIR spectrometer for methane, ethylene and carbon monoxide using a fixed 20m multipass cell, Remote Sensing of Vegetation and Water,

Atmospheric
Measurement
Techniques
Discussions

and Standardization of Remote Sensing Methods, edited by: Cecchi, G., Lamp, T., Reuter, R., and Weber, K., Spie - Int Soc Optical Engineering, Bellingham, 126-136 pp., doi:10.1117/12.274748, 1997.

Laville, P., Jambert, C., Cellier, P., and Delmas, R.: Nitrous oxide fluxes from a fertilised maize crop using micrometeorological and chamber methods, Agric. For. Meteorol., 96, 19-38, doi:10.1016/s0168-1923(99)00054-4, 1999.

5 Lin, C., Liou, N., and Sun, E.: Applications of Open-Path Fourier Transform Infrared for Identification of Volatile Organic Compound Pollution Sources and Characterization of Source Emission Behaviors, J. Air Waste Manage. Assoc., 58, 821-828, doi:10.3155/1047-3289.58.6.821, 2008.

Loh, Z., Chen, D., Bai, M., Naylor, T., Griffith, D., Hill, J., Denmead, T., McGinn, S., and Edis, R.: Measurement of greenhouse gas emissions from Australian feedlot beef production using open-path spectroscopy and atmospheric dispersion modelling, Aust. J. Exp. Agric., 48, 244-247, doi:10.1071/ea07244, 2008.

10 Mosier, A., Wassmann, R., Verchot, L., King, J., and Palm, C.: Methane and Nitrogen Oxide Fluxes in Tropical Agricultural Soils: Sources, Sinks and Mechanisms, Environ. Dev. Sustain., 6, 11-49, doi:10.1023/B:ENVI.0000003627.43162.ae, 2004.

Naylor, T. A., Wiedemann, S. G., Phillips, F. A., Warren, B., McGahan, E. J., and Murphy, C. M.: Emissions of nitrous oxide, ammonia and methane from Australian layer-hen manure storage with a mitigation strategy applied, Anim. Prod. Sci., 56, 1367-1375, 10.1071/an15584, 2016.

15 Ni, K., Koster, J. R., Seidel, A., and Pacholski, A.: Field measurement of ammonia emissions after nitrogen fertilization-A comparison between micrometeorological and chamber methods, Eur. J. Agron., 71, 115-122, doi:10.1016/j.eja.2015.09.004, 2015.

IPCC. Intergovernmental Panel on Climate Change, Fourth Assessment Report-Working I Report: The physical science basis, Cambridge Univ. Press, Cambridge, 2007.

20 Paustian, K., Andren, O., Janzen, H. H., Lal, R., Smith, P., Tian, G., Tiessen, H., Van Noordwijk, M., and Woomer, P. L.: Agricultural soils as a sink to mitigate CO_2 emissions, Soil Use Manage., 13, 230-244, 10.1111/j.1475-2743.1997.tb00594.x, 1997.

Poulsen, T. G., Furman, A., and Liberzon, D.: Effects of Wind Speed and Wind Gustiness on Subsurface Gas Transport, Vadose Zone J., 16, doi:10.2136/vzj2017.04.0079, 2017.

25 Pourbakhtiar, A., Poulsen, T. G., Wilkinson, S., and Bridge, J. W.: Effect of wind turbulence on gas transport in porous media: experimental method and preliminary results, Eur. J. Soil Sci., 68, 48-56, doi:10.1111/ejss.12403, 2017.

Reiche, N., Westerkamp, T., Lau, S., Borsdorf, H., Dietrich, P., and Schütze, C.: Comparative study to evaluate three ground-based optical remote sensing techniques under field conditions by a gas tracer experiment, Environ. Earth Sci., 72, 1435-1441, doi:10.1007/s12665-014-3312-8, 2014.

Rothman, L. S., Jacquemart, D., Barbe, A., Benner, D. C., Birk, M., Brown, L. R., Carleer, M. R., Chackerian, C., Chance, K., Coudert, L. H., Dana, V., Devi, V. M., Flaud, J. M., Gamache, R. R., Goldman, A., Hartmann, J. M., Jucks, K. W., Maki, A. G., Mandin, J. Y., Massie, S. T., Orphal, J., Perrin, A., Rinsland, C. P., Smith, M. A. H., Tennyson, J.,

Tolchenov, R. N., Toth, R. A., Vander Auwera, J., Varanasi, P., and Wagner, G.: The HITRAN 2004 molecular spectroscopic database, J. Quant. Spectrosc. Radiat. Transf., 96, 139-204, doi:10.1016/j.jqsrt.2004.10.008, 2005.

Rochette, P., and Eriksen-Hamel, N. S.: Chamber measurements of soil nitrous oxide flux: are absolute values reliable?, Soil Sci. Soc. Am. J., 72, 331-342, doi: 10.2136/sssaj2007.0215, 2008.

Rowlings, D. W., Grace, P. R., Kiese, R., and Weier, K. L.: Environmental factors controlling temporal and spatial variability in the soil-atmosphere exchange of CO_2, CH_4 and N_2O from an Australian subtropical rainforest, Glob. Change Biol., 18, 726-738, doi:10.1111/j.1365-2486.2011.02563.x, 2012.

Russwurm, G. M., Kagann, R. H., Simpson, O. A., and McClenny, W. A.: Use of a fourier-transform spectrometer as a remote sensor at superfund sites, Proc. SPIE 1433, Measurement of Atmospheric Gases, 302-314, doi: 10.1117/12.46177, 1991.

Russwurm, G. M., Kagann, R. H., Simpson, O. A., McClenny, W. A., and Herget, W. F.: Long-path FTIR measurements of volatile organic-compounds in an industrial-setting, J. Air Waste Manage. Assoc., 41, 1062-1066, doi:10.1080/10473289.1991.10466900, 1991.

Russwurm, G. M., and Childers, J. W.: FT-IR open-path monitoring guidance document, ManTech Environmental Technology, Inc., Research Triangle Park, NC (United States), 1996.

Ryden, J. C., and Lund, L. J.: Nitrous Oxide Evolution from Irrigated Land[1], J. Environ. Qual., 9, doi:10.2134/jeq1980.00472425000900030012x, 1980.

Schelde, K., Cellier, P., Bertolini, T., Dalgaard, T., Weidinger, T., Theobald, M. R., and Olesen, J. E.: Spatial and temporal variability of nitrous oxide emissions in a mixed farming landscape of Denmark, Biogeosciences, 9, 2989-3002, doi:10.5194/bg-9-2989-2012, 2012.

Shao, L., Pollard, M. J., Griffiths, P. R., Westermann, D. T., and Bjorneberg, D. L.: Rejection criteria for open-path Fourier transform infrared spectrometry during continuous atmospheric monitoring, Vib. Spectrosc., 43, 78-85, doi:10.1016/j.vibspec.2006.06.016, 2007.

Smith, P.: Carbon sequestration in croplands: the potential in Europe and the global context, Eur. J. Agron., 20, 229-236, doi:10.1016/j.eja.2003.08.002, 2004.

Smith, P., Martino D., Cai Z., Gwary D., Janzen H., Kumar P., McCarl B., Ogle S., O'Mara F., Rice C., Scholes B., and Sirotenko O.: Agriculture. In B. Metz et al. (ed.) Mitigation. Contribution of Working Group III to the fourth assessment report of the Intergovernmental Panel on Climate Change. Cambridge Univ. Press, Cambridge, UK, 2007.

Smith, P., Martino, D., Cai, Z., Gwary, D., Janzen, H., Kumar, P., McCarl, B., Ogle, S., O'Mara, F., Rice, C., Scholes, B., Sirotenko, O., Howden, M., McAllister, T., Pan, G., Romanenkov, V., Schneider, U., Towprayoon, S., Wattenbach, M., and Smith, J.: Greenhouse gas mitigation in agriculture, Philos. Trans. R. Soc. B-Biol. Sci., 363, 789-813, doi:10.1098/rstb.2007.2184, 2008.
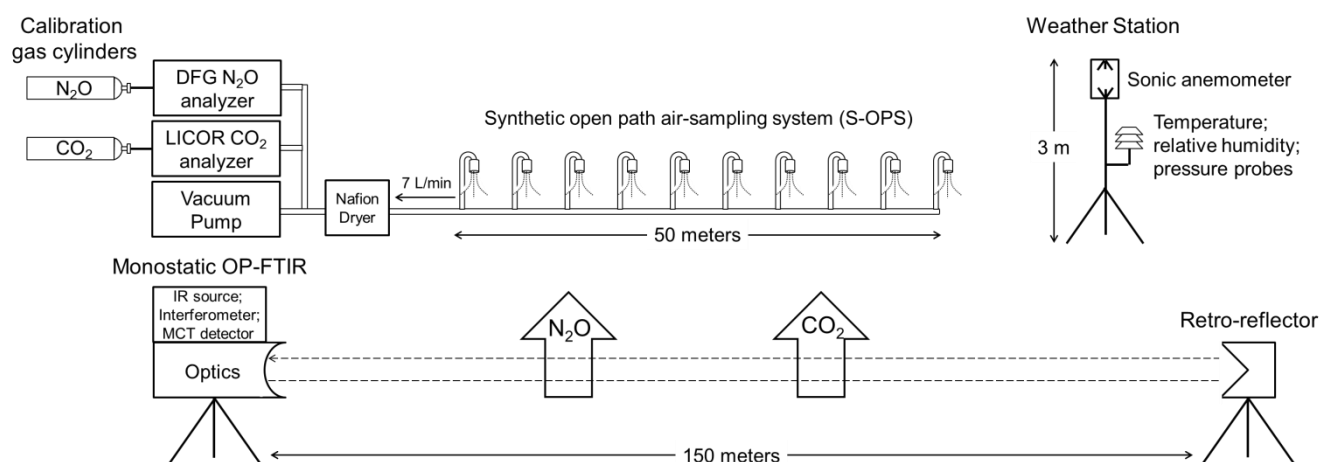
Smith, T. E. L., Wooster, M. J., Tattaris, M., and Griffith, D. W. T.: Absolute accuracy and sensitivity analysis of OP-FTIR retrievals of CO_2, CH_4 and CO over concentrations representative of "clean air" and "polluted plumes", Atmos. Meas. Tech., 4, 97-116, doi:10.5194/amt-4-97-2011, 2011.

US-EPA: Global Anthropogenic Emissions of Non-CO_2 Greenhouse Gases: 1990-2020, United States Environmental
5   Protection Agency, EPA 430-R-06-003, Washington, D.C., <https://www.epa.gov/sites/production/files/2016-05/documents/globalanthroemissionsreport.pdf>, 2006.

West, T. O., and McBride, A. C.: The contribution of agricultural lime to carbon dioxide emissions in the United States: dissolution, transport, and net emissions, Agric. Ecosyst. Environ., 108, 145-154, doi:10.1016/j.agee.2005.01.002, 2005.

10

Figure 1. Schematic of the instrumentation used to assess the accuracy of N_2O and CO_2 concentration determined by OP-FTIR in this study. DFG N_2O and LI-840 CO_2 analyzers combined with the synthetic open path air-sampling system (S-OPS) were used to measure the
15   'actual' path-averaged N_2O/CO_2 concentrations and benchmark the N_2O and CO_2 concentrations calculated from OP-FTIR spectral analyses. The humidity, air temperature, and wind information were measured from the weather station.
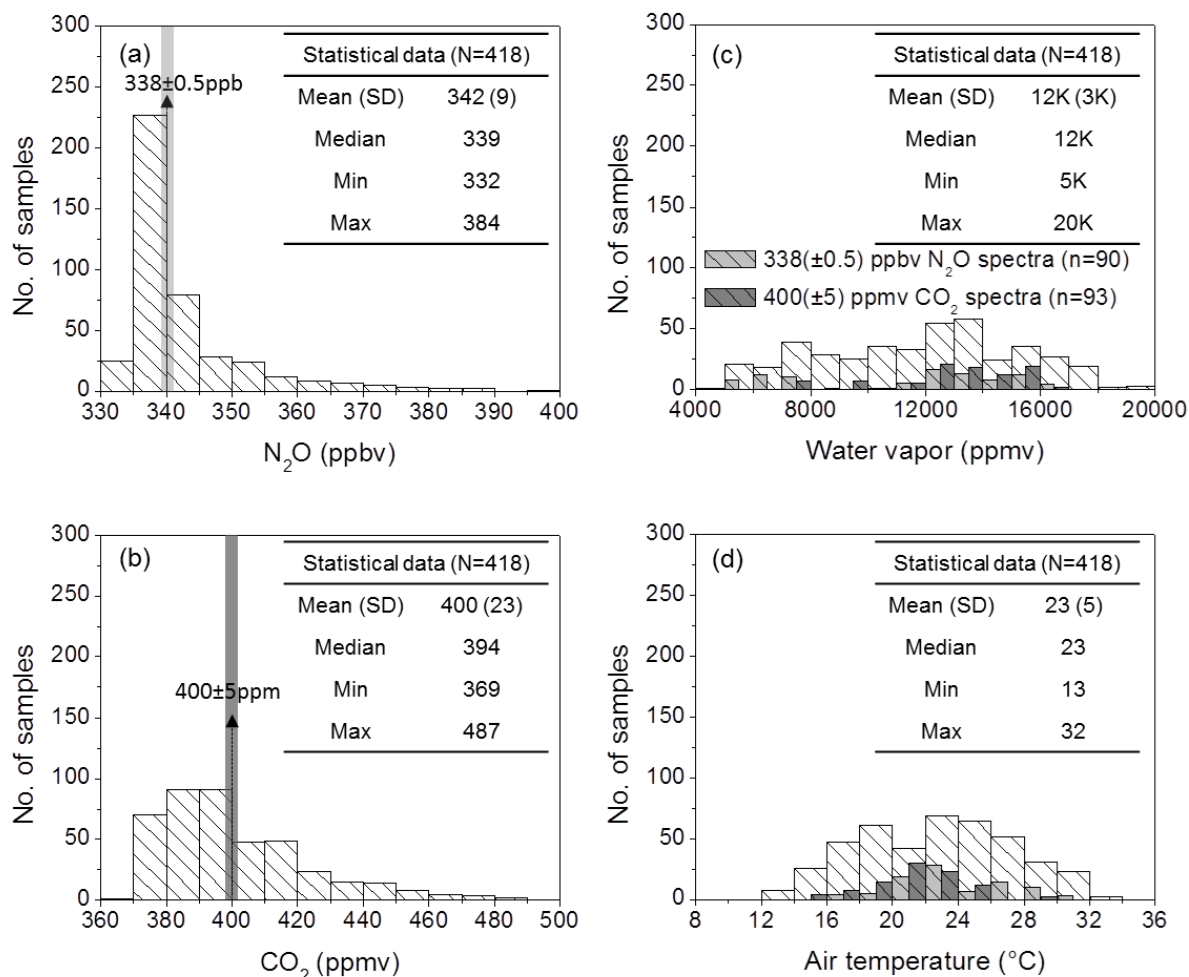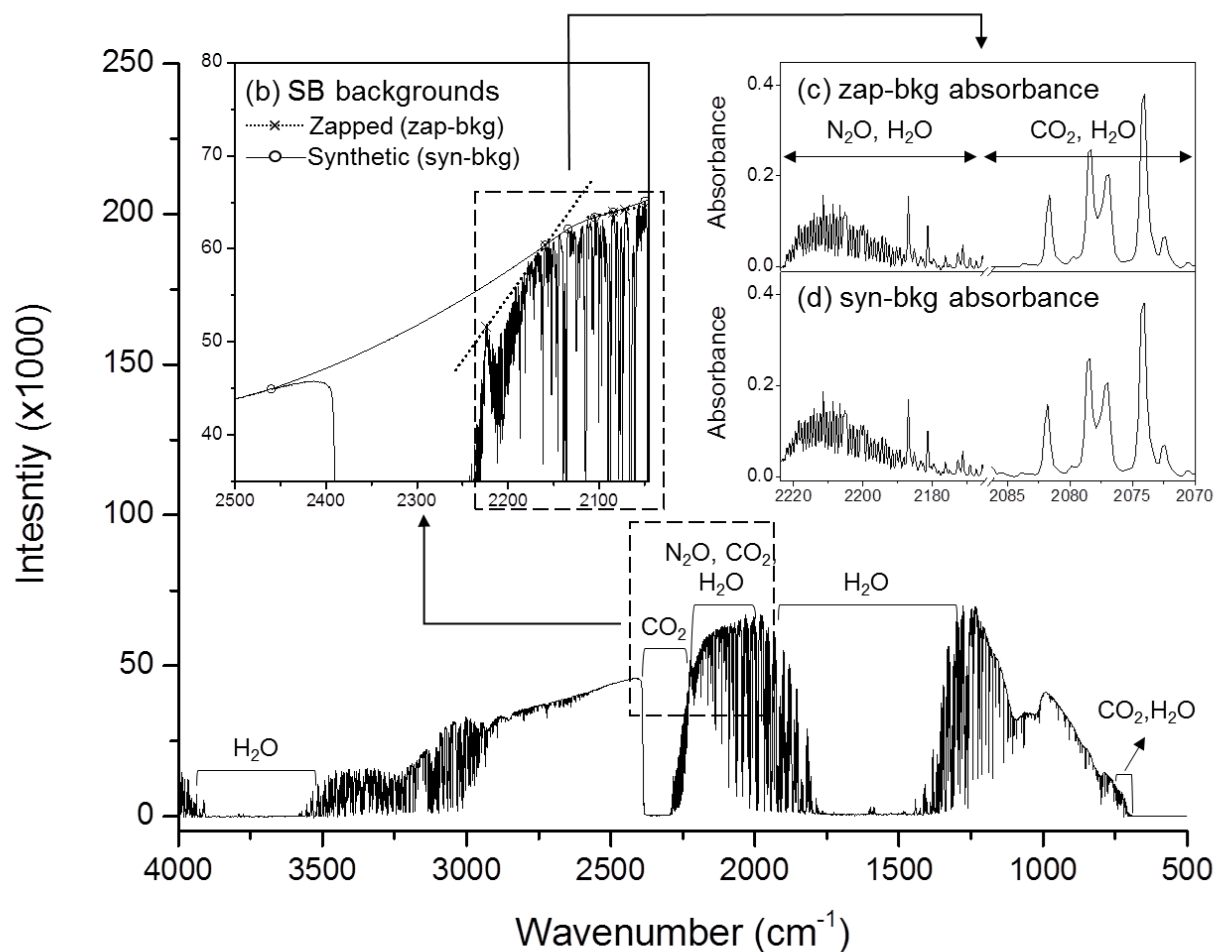
Figure 2. The 30-min averaged concentrations of (a) N_2O and (b) CO_2 were measured using N_2O and CO_2 analyzers by sampling the air from S-OPS, and the 30-min averages of (c) water vapour content and (d) air temperature were also measured from the on-site weather station during 9th-19th in June, 2014. The concentrations of N_2O, CO_2, and water vapour showed in these figures were measured while the air was well-mixing (U > 1.7 m·s^{-1}). The light gray bars mean the OP-FTIR spectra containing 338(±0.5) ppbv N_2O and the dark gray barks mean the OP-FTIR spectra containing 400(±5) ppmv CO_2. Both the selected spectra (N_2O 338 ppbv, n=90; CO_2 400 ppmv, n=93) covered the broad ranges of water vapour and air temperature and were used to assess the sensitivity of the OP-FTIR quantitative methods to the dynamic ambient factors.

17

Figure 3. The illustrations of (a) a field single beam (SB) OP-FTIR spectrum containing the regions of N_2O, CO_2, and water vapour was collected through an optical path length of 300 m; (b) a zapped and a synthetic SB backgrounds (zap-bkg and syn-bkg) were generated from this field SB spectrum and used to convert the sampled SB spectrum to (c) the absorbance spectra that allow us to calculate N_2O/CO_2 concentrations using Beer-Lambert law.
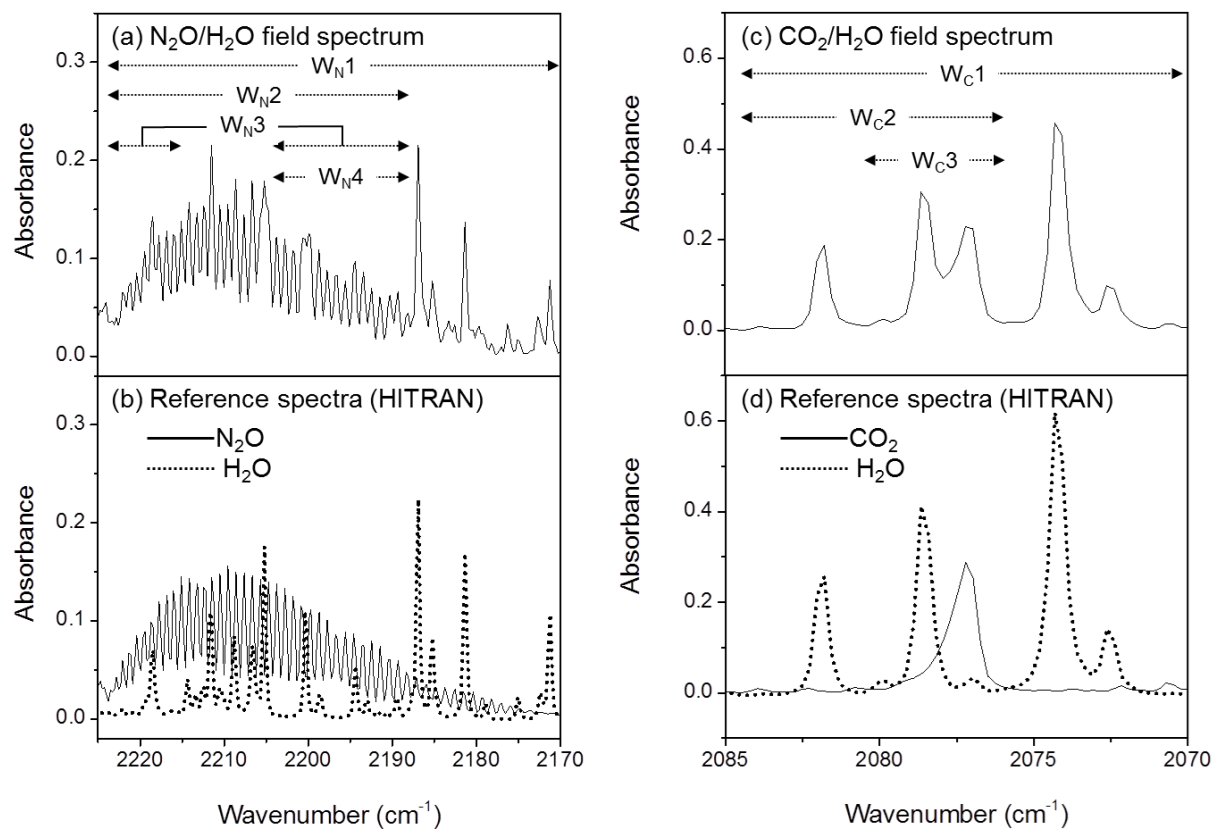
Atmospheric
Measurement
Techniques
Discussions

Figure 4. Field and HITRAN reference absorbance spectra: (a) Field spectrum containing the features of N_2O and water vapour, (b) reference spectra of N_2O and water vapour at 2170 - 2225 cm^{-1}, (c) field spectrum containing the features of CO_2 and water vapour, and (d) reference spectra of CO_2 and water vapour at 2070 - 2085 cm^{-1}. W_N(1-4) and W_C(1-3) denote the spectral windows used to calculate N_2O and CO_2 concentrations from field spectra.
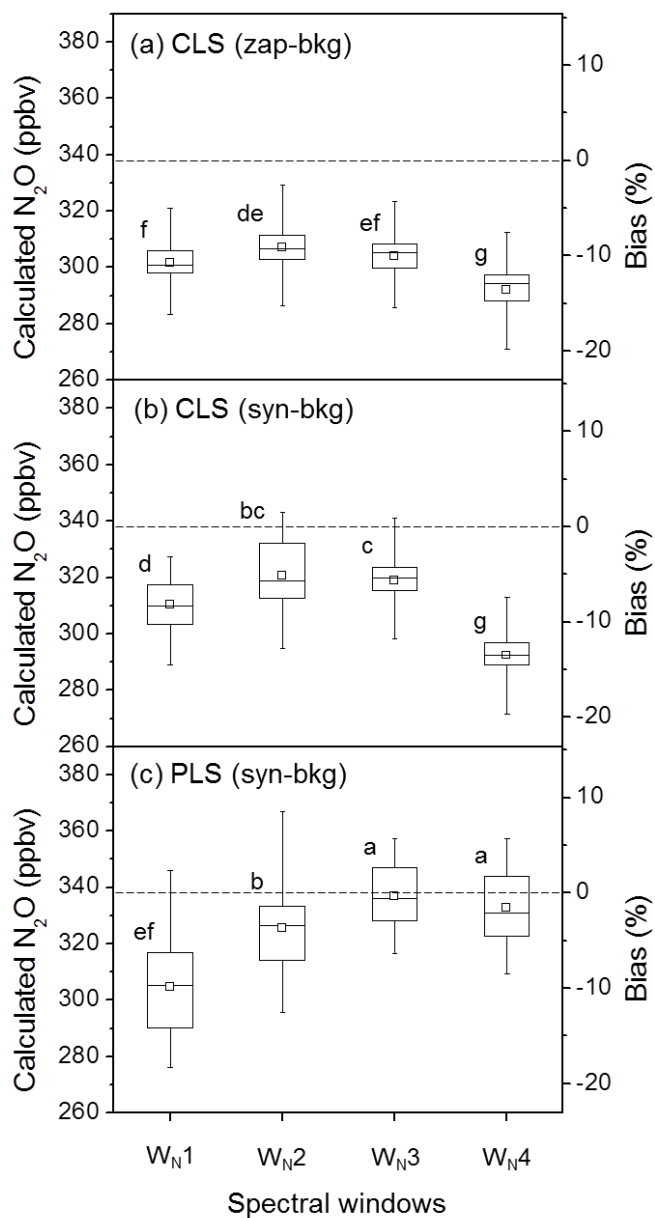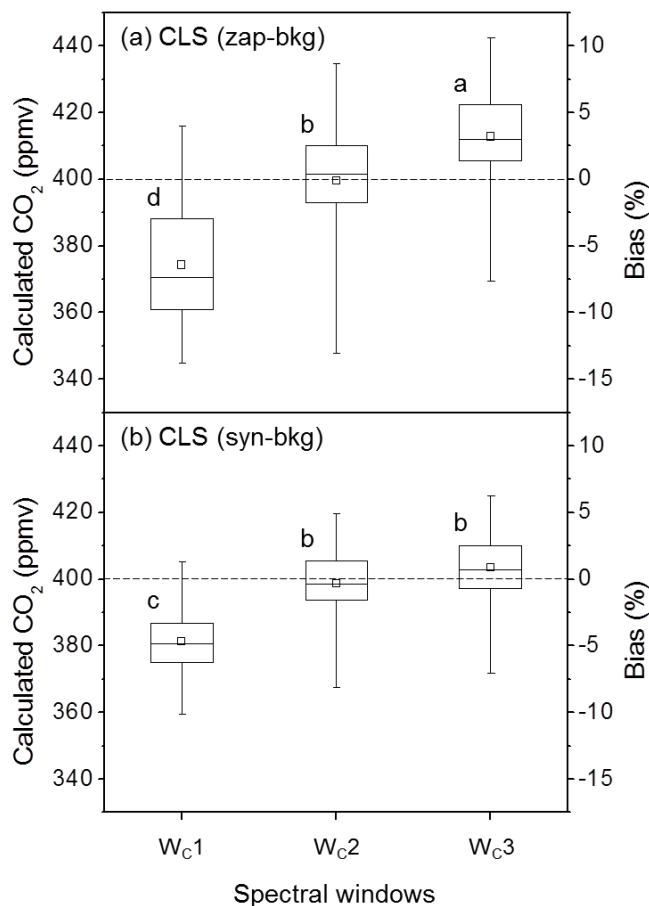
Figure 5. The box plots of the calculated N_2O concentrations and the corresponding biases from a series of OP-FTIR spectra (n=90) that contain 338 ppbv N_2O with the changed humidity and air temperature using different SB background-processing methods (i.e. zap-bkg and syn-bkg), and four spectral windows (W_N1-4) in the CLS and PLS models: (a) zap-bkg + CLS model, (b) syn-bkg + CLS model, and (c) syn-bkg + PLS model. The plot displays the mean (□), median (—), interquartile ranges (box), and extreme values (whiskers). Different letters indicate the significant difference (P < 0.05) among the means calculated by different quantitative methods by the least significant difference (LSD).

Figure 6. The box plots of the calculated CO_2 concentrations and the corresponding biases from a series of OP-FTIR spectra (n=93) that contain 400 ppmv CO_2 with the changed humidity and air temperature using different SB background-processing methods (i.e. zap-bkg and syn-bkg), and three spectral windows (W_C1-3) in the CLS model: (a) zap-bkg, and (b) syn-bkg. The plot displays the mean ($\square$), median (—), interquartile ranges (box), and extreme values (whiskers). Different letters indicate the significant difference (P < 0.05) among the means calculated by different quantitative methods by the least significant difference (LSD).
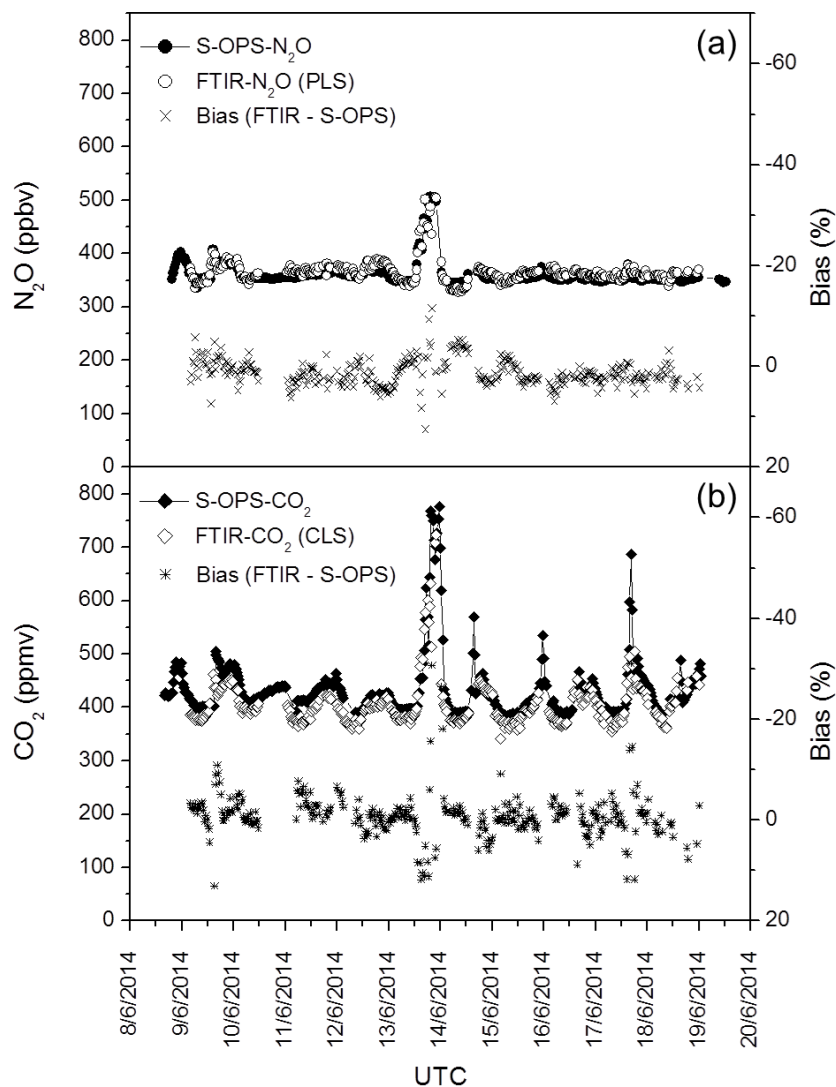
Figure 7. N_2O and CO_2 concentrations from 9th to 19th in June 2014: (a) N_2O concentrations measured from S-OPS using the DFG N_2O analyzer and calculated from OP-FTIR using the optimal methods (syn-bkg + W_N3 + the PLS model), and the corresponding biases, and (b) CO_2 concentrations measured from S-OPS using LI-840 CO_2 analyzer and calculated from OP-FTIR using the optimal method (syn-bkg + W_C2 + the CLS model), and the corresponding bias.